journal

J. Am. Ceram. Soc., 94 [12] 4340–4344 (2011)
DOI: 10.1111/j.1551-2916.2011.04699.x

Phase Transformation Behavior and Electrical Properties of $Pb(Zr_{0.56}Ti_{0.44})O_3$–$Bi(Zn_{0.5}Ti_{0.5})O_3$ Solid Solution Ceramics

Ruzhong Zuo,[‡,†] Yi Liu,[‡] Shi Su,[‡] Xiangcheng Chu,[§] and Xiaohui Wang,[§]

[‡]School of Materials Science and Engineering, Institute of Electro Ceramics and Devices, Hefei University of Technology, Hefei, 230009, China

[§]State Key Lab of New Ceramics and Fine Processing, Department of Materials Science and Engineering, Tsinghua University, Beijing, 100084, China

The solid solutions of $(1-x)Pb(Zr_{0.56}Ti_{0.44})O_3$–$xBi(Zn_{0.5}Ti_{0.5})O_3$ ($(1-x)PZ_{56}T_{44}$–$xBZT$) were synthesized via a solid-state reaction method. X-ray diffraction results indicated that the tetragonality of $(1-x)PZ_{56}T_{44}$–$xBZT$ was enhanced with increasing the BZT content, and a morphotropic phase boundary (MPB) between rhombohedral and tetragonal ferroelectric phases was identified to be in the range of $0.15 < x < 0.18$. In addition, the dielectric diffuseness and frequency dispersion behavior were induced with increasing the BZT content, owing to increased disorder degree of both A-site and B-site cations in $(1-x)PZ_{56}T_{44}$–$xBZT$ perovskite lattice. Contrary to the case in PT–BZT, the increased tetragonality accompanies reduced Curie temperatures (T_c) as $PZ_{56}T_{44}$ was substituted by BZT. The electrical properties of solid solutions exhibit obviously compositional dependence. The optimum dielectric and piezoelectric properties of $\varepsilon_{33}^T = 1430$, $d_{33} = 365$ pC/N, $k_p = 50\%$, $Q_m = 32$, and $T_c = 260$°C were achieved in $(1-x)PZ_{56}T_{44}$–$xBZT$ ceramics with $x = 0.18$ owing to the co-existence of two ferroelectric phases near the MPB.

I. Introduction

Lead-based perovskite structured binary piezoelectric ceramics, such as $PbZrO_3$–$PbTiO_3$ (PZT), have been widely used for their high piezoelectric coefficients and large electromechanical coupling factors.[1,2] The high piezoelectric activity should be achieved near a morphotropic phase boundary (MPB) where two perovskite ferroelectric phases with different lattice distortions coexist.[3,4] To further improve piezoelectric properties, some ternary solid solutions with a new MPB have been successfully developed, consisting of PZT and lead-based complex perovskite ferroelectrics such as $Pb(Me_{1/3}Nb_{2/3})O_3$-type (where Me–Mg^{2+}, Zn^{2+}, Ni^{2+}, etc.), because these ferroelectrics might have extremely high dielectric activity.[5–7] As far as the lead pollution to the environment is concerned, lead-free and low-lead piezoelectric ceramics have attracted much attention in the past few years. Unfortunately, currently focused lead-free ferroelectric systems such as titanate- or niobate-based compositions have exhibited either processing difficulties or stability issues of piezoelectric properties,[8] which could make them quite hard to be applied in industry. In contrast, it should be meaningful and applicable to develop lead-reduced piezoelectric ceramics to satisfy the requirements of industry.

Bismuth-based perovskite compounds such as $BiMeO_3$ (Me: Fe^{3+}, Sc^{3+}, $Ni_{1/2}Ti_{1/2}$, $Mg_{1/2}Ti_{1/2}$, $Ni_{2/3}Nb_{1/3}$, and $Zn_{1/2}Ti_{1/2}$, etc.) are typical lead-free ferroelectrics and have been largely investigated experimentally[9–15] and theoretically[16–18] in recent years. As a new member of ABO_3 perovskite family, it seems that almost all Bi-based perovskites possess $BiFeO_3$- or $GdFeO_3$-type distorted perovskite structure,[14,15,19] but unique behavior has been observed in Zn-containing Bi-based perovskite compounds, for example, $Bi(Zn_{0.5}Ti_{0.5})O_3$ (BZT). It has been reported that BZT should be synthesized under high pressure and shows a tetragonal PT-type structure with random Zn/Ti distribution and a high c/a ratio of 1.211 but a low tolerance factor ($t = 0.95$).[14] The large tetragonality of BZT could be stabilized by the interaction of covalent bonds and the coupling between the tetragonal distortion of unite cell and internal atomic off-center displacement,[17] resulting in some unique properties, such as large polarization and high Curie temperature T_c.[18] Therefore, BZT could be a potential tetragonal perovskite material. In addition, diffuse ferroelectric phase transformation behavior probably exists in BZT, since it was usually observed in A-site or B-site complex perovskites. Unfortunately, its T_c was predicted to be higher than its decomposition and synthesis temperature.[14] As a result, there has been so far lack of direct evidences for whether BZT has a relaxor ferroelectric behavior. However, some hints have been observed in BZT-containing solid solutions with PT, $BaTiO_3$ (BT), $(Bi_{1/2}K_{1/2})TiO_3$ (BKT), $(Bi_{1/2}Na_{1/2})TiO_3$ (BNT), and $(K_{0.5}Na_{0.5})NbO_3$ (KNN),[20–24] in which pronounced relaxor ferroelectric behavior was observed with increasing BZT content. Accordingly, BZT could be an interesting alternative to some lead-based relaxor ferroelectrics for the purpose of composing ternary solid solutions with PZT. Although BZT–PZT solid solutions were prepared for various purposes,[25–29] yet a full study on their phase transformation behavior, ferroelectric phase characteristics, and compositional dependence of piezoelectric properties has been still missing.

Considering that Zr-rich compositions in PZT own a rhombohedral symmetry, it is thus expected that an MPB would be observed between the Zr-rich PZT and BZT. The purpose of this work is then to identify how the phase structure of $Pb(Zr_{0.56}Ti_{0.44})O_3$ ($PZ_{56}T_{44}$) changes with the BZT content and simultaneously to explore the sintering behavior and electrical properties of $(1-x)PZ_{56}T_{44}$–$xBZT$ solid solution ceramics. The compositional and structural dependencies of various electrical properties are discussed. Particular attention was paid to the ferroelectric phase transition behavior of solid solution ceramics.

C. A. Randall—contributing editor

Manuscript No. 29387. Received February 28, 2011; approved May 19, 2011.

This work was financially supported by a project of Natural Science Foundation of Anhui Province (090414179), and by the National Natural Science Foundation of China (50972035), a Program for New Century Excellent Talents in University, State Education Ministry (NCET-08-0766) and a 973 Program (No. 2009CB623301).

[†]Author to whom correspondence should be addressed. e-mail: piezolab@hfut.edu.cn

II. Experimental Procedure

The solid-solution ceramics $(1-x)PZ_{56}T_{44}$–xBZT (x = 0.05–0.25) was prepared via a conventional solid-state reaction method using high-purity oxides: Bi_2O_3 ($\geq$99.0%), ZnO ($\geq$99.0%), TiO_2 ($\geq$99.0%), PbO ($\geq$99.0%), and ZrO_2 ($\geq$99.0%) as raw materials. After mixing, the powder mixtures were calcined in a closed alumina crucible at 850°C for 3 h in air. The calcined powder was then milled again for 20 h together with 0.5% PVB binder in a planetary mill using 3 mm yttria-stabilized zirconia balls. After drying, the powder was uniaxially pressed into pellets of approximately 10 mm in diameter and 1 mm in thickness. Sintering was carried out in the temperature range of 1000°C–1080°C for 2 h in double alumina crucibles. To minimize the vaporization of Bi and Pb, sample disks were buried in the sacrificial powder of the same composition. For electrical measurements, silver paste was painted on major sides of the samples and then fired at 550°C for 30 min. The samples were poled at 110°C in a silicone oil bath under a dc electric field of 3–4 kV/mm for 15 min.

The phase structures were analyzed at room temperature by an X-ray diffractometer (XRD, D/Max-RB; Rigaku, Tokyo, Japan) using Cu$K\alpha$1 radiation. The microstructure was observed using a scanning electron microscope (SEM, JEOL JSM-6490LV, Tokyo, Japan). Dielectric properties were measured as a function of temperature by an LCR meter (Agilent E4980A, Santa Clara, CA). Polarization vs electric field (P–E) hysteresis loops were measured using a ferroelectric measuring system (Precision LC, Radiant Technologies Inc., Albuquerque, NM). The piezoelectric strain constant d_{33} of poled samples was measured by a Belincourt-meter (YE2730A; Sinocera, Yangzhou, China). The planar electromechanical coupling factor k_p and the mechanical quality factor Q_m were determined by a resonance–antiresonance method with an impedance analyzer (PV70A; Beijing Band ERA Co. Ltd., Beijing, China).

III. Results and Discussion

The XRD patterns of $(1-x)PZ_{56}T_{44}$–xBZT ceramics are shown in Fig. 1. All major peaks could be assigned to perovskite-structured phases. It can be seen that diffraction peaks for secondary phases gradually appear for compositions with $x \geq 0.20$, which can be indexed as $Bi_{12}TiO_{20}$ (PDF No. 42-0186). The basic reason can be attributed to the solubility limit of BZT in $PZ_{56}T_{44}$. Moreover, a low tolerance factor (t = 0.95) of BZT tends to induce the instability of the perovskite structure of solid solutions with increasing its content. The asymmetric (111) peaks and non-split (001) peaks suggest that compositions $x \leq 0.14$ may own a rhombohedral structure. As x = 0.2, the asymmetry of (111) peak is absent and simultaneously (001) and (002) peaks are split, generally indicating the presence of a tetragonal phase. For compositions with x = 0.15–0.18, (002)/(200) peaks were found to gradually separate from each other, indicating that two-phase coexistence zone occurs in this composition range. That is to say, with increasing BZT content x, the solid solutions undergo a transition from a single rhombohedral phase, to a mixture of rhombohedral and tetragonal phases and finally to a pure tetragonal phase. An MPB separating rhombohedral and tetragonal phases should be thus identified to be in the range of x = 0.15–0.18. This can be more clearly observed by calculating the lattice parameters of $(1-x)PZ_{56}T_{44}$–xBZT ceramics through fitting the diffraction peak profiles, as shown in Fig. 2. It is clear that there is a transition zone between the rhombohedral and the tetragonal phase in the range of $0.15 < x < 0.18$. It can be seen that the addition of BZT tends to increase the tetragonality of the system. The c/a value for the composition with x = 0.18 is 1.012 increases to 1.026 for x = 0.25. The increase in tetragonality is similar to previous results in the BZT–PT solid solutions where it was believed that the enhancement of tetragonality results from the strong coupling between A-site Pb/Bi cations and B-site ferroelectrically active cations such as Ti^{4+} and Zn^{2+}.[30] On the one hand, ferroelectrically active ions can form short, covalent bonds with oxygen; on the other hand, large Bi^{3+} displacements and A–B site displacement coupling would necessitate a large B-site displacement. These two characteristics would stabilize the tetragonal perovskite phases.[31]

Figure 3 shows the SEM micrographs of $(1-x)PZ_{56}T_{44}$–xBZT ceramics sintered at 1025°C for 2 h. It can be seen that the increase of BZT content has only slight effect on the grain size and morphology of $(1-x)PZ_{56}T_{44}$–xBZT ceramics but a clear effect on the densification behavior. The average grain size for samples sintered at 1025°C varies in the range of 1.6–2.7 μm. The SEM photos indicate that the sintered density becomes lower with increasing BZT content. Compared to a pure $PZ_{56}T_{44}$,[1] the addition of a small amount of BZT tends to promote its densification. For example, a relative density of >96% can be achieved in $0.82PZ_{56}T_{44}$–0.18BZT ceramic as it was sintered only at 1025°C. The reason is basically due to the fact that both Bi and Zn are usually effective sintering aids. However, as the BZT content is high, the appearance of a small amount of secondary phases might contribute to the inhibition of grain growth and the degradation of densification based on the pinning effect of grain boundary.

Dielectric constant as a function of temperature for unpoled $(1-x)PZ_{56}T_{44}$–xBZT (x = 0.05–0.20) ceramics sintered at optimum temperatures is shown in Fig. 4. It can be found that both the dielectric maxima and T_c values decrease with increasing the BZT content. However, the dielectric constant

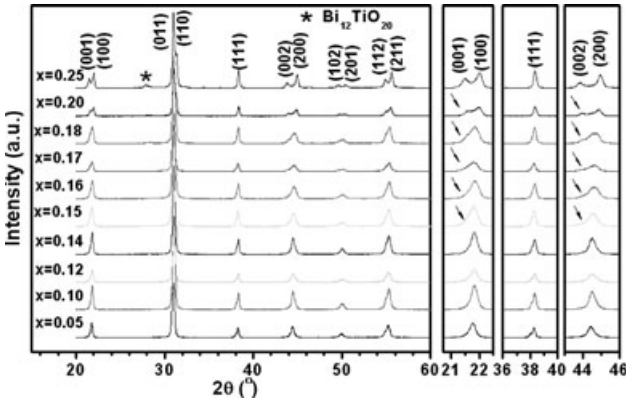

Fig. 1. X-ray diffraction patterns at room temperature for sintered $(1-x)PZ_{56}T_{44}$–xBZT ceramics as indicated.

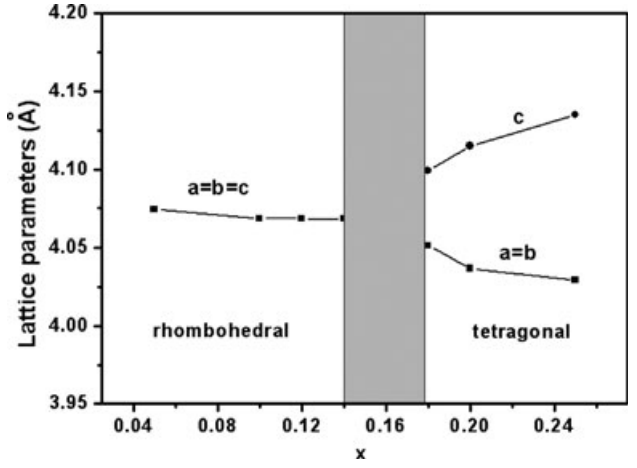

Fig. 2. The lattice parameters for $(1-x)PZ_{56}T_{44}$–xBZT ceramics as a function of the BZT content.

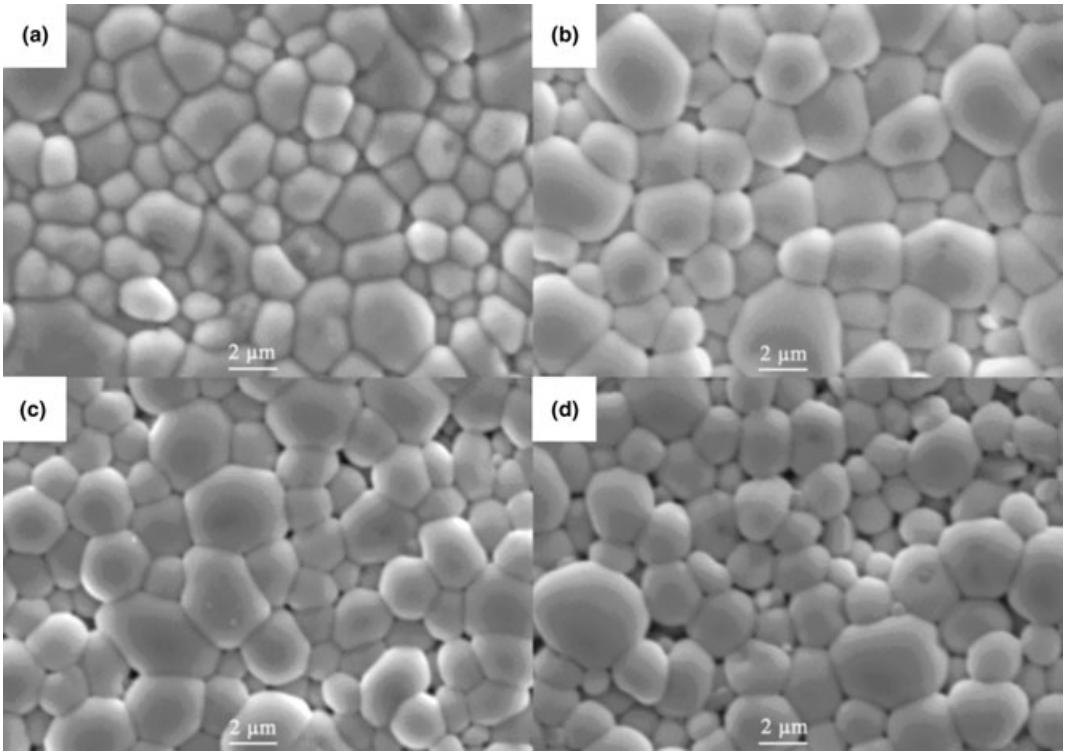

Fig. 3. Scanning electron microscopy images of $(1-x)PZ_{56}T_{44}$–xBZT ceramics sintered at 1025°C for 2 h: (a) $x = 0.12$, (b) $x = 0.18$, (c) $x = 0.20$, and (d) $x = 0.25$.

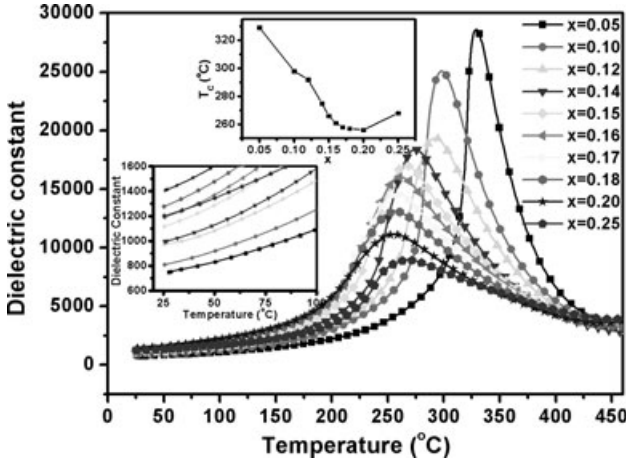

Fig. 4. Dielectric constant at 1 kHz as a function of temperature for $(1-x)PZ_{56}T_{44}$–xBZT solid solutions sintered at optimal temperatures.)

at room temperature increases with x as can be seen from the inset of Fig. 4. A slight increase of T_c and a small decrease of room-temperature dielectric constant for the composition with $x = 0.25$ is probably due to the existence of secondary phases. Contrary to PT–BZT,[20] $(1-x)PZ_{56}T_{44}$–xBZT ($x \leq 0.20$) ceramic exhibits a decreased T_c with the addition of BZT. However, it is similar to BZT–PZ system.[32] A decline in T_c usually corresponds to a decrease in tetragonality for a couple of perovskite solid solution ceramics, such as PZT, $Pb(Mg_{1/3}Nb_{2/3})O_3$–PT, and $Bi(Me)O_3$–PT systems.[20,33–36] In $Bi(Me)O_3$–PT systems, it has been proposed that the large tetragonal distortions and associated high T_c could be attributed to a strong coupling between the A-site and B-site off-center distortions when B-site positions are completely occupied by ferroelectrically active cations such as Zn^{2+}, Ti^{4+}, and Fe^{3+}.[20,31] It seems that while the addition of BZT tends to enhance the tetragonality but why it reduces T_c in PZT systems cannot be well explained in the same way. The possible reason may be ascribed to the presence of Zr^{4+} which is not ferroelectrically active.[32] In addition, the same effect was found in $K_xNa_{1-x}NbO_3$–$LiSbO_3$ system where the increase of tetragonality accompanies a decrease of T_c.[37,38]

In addition to the decrease of T_c, the ferroelectric phase transition zone was found to become broader and broader with increasing the BZT content. As an example, the dielectric properties as a function of temperature and frequency for $0.82PZ_{56}T_{44}$–0.18BZT ceramics are shown in Fig. 5(a). It is evident that with increasing the measuring frequency, the T_c or T_m value (at the position of the dielectric maxima) increases accordingly. The same change can be also seen from the change of loss tangent value with frequency. On the other hand, the dielectric diffusivity can be clearly found in most of BZT substituted $PZ_{56}T_{44}$ ceramics. The diffuseness of the phase transition can be determined from the modified Curie–Weiss law,[39] which can be expressed as $1/\varepsilon - 1/\varepsilon_m = C^{-1}(T-T_m)^{\gamma}$ where γ is the degree of diffuseness, C is the Curie–Weiss constant, and T_m is the phase transition temperature corresponding to the maximum dielectric constant ε_m. The parameter γ varies in the range from 1 for a normal ferroelectric to 2 for an ideal relaxor ferroelectric. The γ values for different compositions can be determined from the slopes of linearly fitted lines as shown in Fig. 5(b). Three compositions ($x = 0.12$, 0.18, and 0.2) were chosen as examples, which belong to the rhombohedral phase, MPB and the tetragonal phase, respectively. Clearly, the diffuse phase transition characteristics and frequency dispersion phenomenon at T_m can be observed in all three samples. The relaxor behavior in ferroelectrics was well explained using the viewpoint of polar nanoregions (PNRs) as a result of the local electric fields and elastic fields.[40,41] In the solid solution of $(1-x)PZ_{56}T_{44}$–xBZT, Bi^{3+} (1.36 Å, CN = 12) possesses different valences and ionic radii from Pb^{2+} (1.49 Å, CN = 12),[42] and both of them occupy the A site of ABO_3 perovskite structure. As a result, local

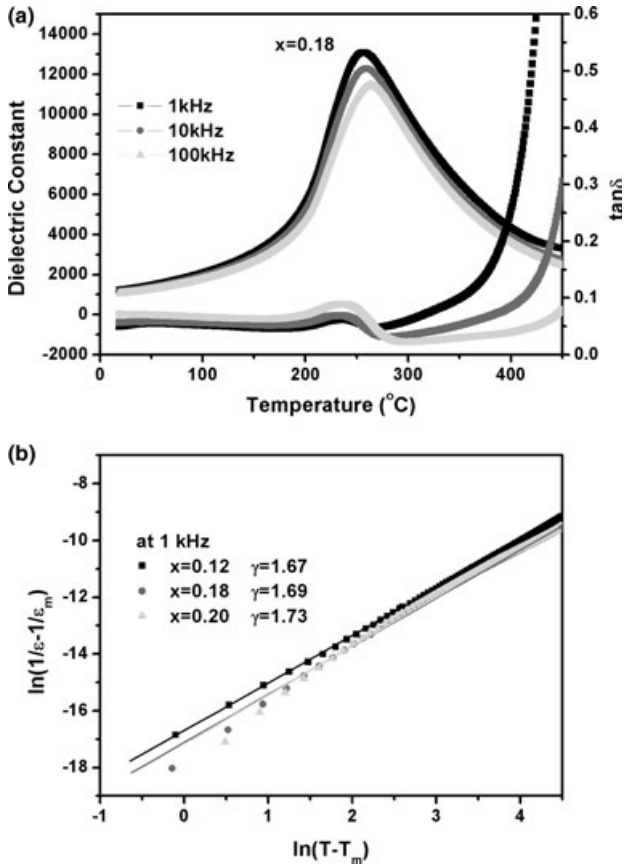

Fig. 5. (a) Temperature and frequency dependence of dielectric constant and dielectric loss for $(1-x)PZ_{56}T_{44}$–xBZT ceramics with $x = 0.18$ and (b) a plot of $\ln(1/\varepsilon - 1/\varepsilon_m)$ vs $\ln(T - T_m)$ for $(1-x)PZ_{56}T_{44}$–xBZT ceramics with $x = 0.12$, 0.18, and 0.20, respectively.

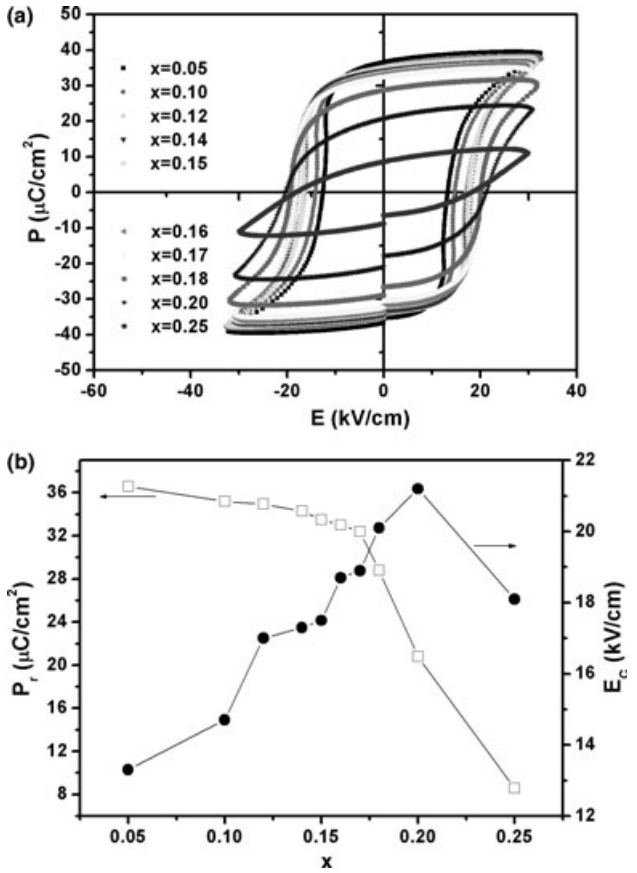

Fig. 6. (a) Polarization vs electric field hysteresis loops (10 Hz) of $(1-x)PZ_{56}T_{44}$–xBZT ceramics sintered at optimal temperatures and (b) remnant polarization P_r and coercive field E_c of $(1-x)PZ_{56}T_{44}$–xBZT ceramics as a function of the BZT content.

electric fields would be formed owing to the different electrical charges of Pb^{2+} and Bi^{3+} and the local elastic fields formed due to local structure distortions induced by the different ionic radii. The similar phenomenon would be observed at the B site where Ti^{4+} (0.605 Å, CN = 6), Zr^{4+} (0.72 Å, CN = 6), and Zn^{2+} (0.74 Å, CN = 6)[42] also possess different electrical charges and ionic sizes. The presence of the random fields thus gives rise to the PNRs by disturbing the long-range dipole alignment.[40] The relaxor behavior can be considered as the complex response of all PNRs and disordered matrix. The concentration of random fields increases with the increase of the cation disorder degree at both A-sites and B-sites ions and results in an increased number of PNRs consequently. Therefore, it can be understood that the relaxor behavior of $(1-x)PZ_{56}T_{44}$–xBZT ceramics was enhanced with the increase of BZT content.

The ferroelectricity of $(1-x)PZ_{56}T_{44}$–xBZT ceramics was characterized by measuring P–E hysteresis loops at 10 Hz, as shown in Fig. 6. From Fig. 6(a), the remnant polarization (P_r) and coercive field (E_c) values are plotted against BZT content x in Fig. 6(b). It can be seen that well-saturated hysteresis loops were obtained over a wide composition range. With increasing the BZT content, E_c increases but P_r decreases. A larger E_c value at BZT-rich side should be in general attributed to the increased tetragonality, owing to a higher strain associated with 90° domain rotation. The E_c value for the sample with $x = 0.25$ seems to decrease probably because it was obtained from a poorly saturated loop owing to a relatively high leakage current caused by relatively low sample density. In addition, the existence of non-ferroelectric secondary phase would also make the loop slimmer. Interestingly, the optimum P_r value

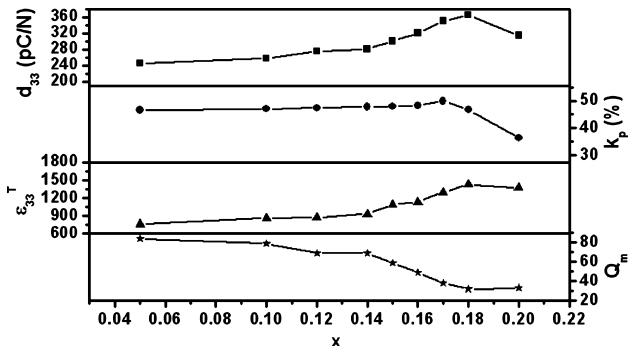

Fig. 7. Dielectric and piezoelectric properties of poled $(1-x)PZ_{56}T_{44}$–xBZT ceramics as a function of the BZT content.

does not appear near MPB compositions ($x = 0.15$–0.18). In general, enhanced ferroelectric property could be observed at MPB owing to the coexistence of rhombohedral and tetragonal phases with 14 possible directions. It means that the effect of the phase coexistence on ferroelectricity was probably compromised by the reduced T_c values with increasing BZT content. Within the tetragonal region, the decreased T_c indicates a destabilization of the ferroelectric phase.[21]

Figure 7 shows the dielectric and piezoelectric properties for poled $(1-x)PZ_{56}T_{44}$–xBZT ceramics sintered at optimum temperatures. Owing to the appearance of secondary phases, the composition with $x = 0.25$ was not discussed herein. It can be seen that the dielectric and piezoelectric properties exhibit obviously compositional dependences. They first gradually increase with x, and then reach the maxima

approximately at $x = 0.18$ and finally start to decline. Therefore, it is obvious that the MPB plays an important role in improving the electrical properties. The enhanced piezoelectric properties are mostly associated with the improved dielectric activity, as explained by a simple relation: $d_{33} = 2Q_{11}\varepsilon P_s$ where Q_{11} is the electrostrictive coefficient, ε is the dielectric constant, and P_s is the spontaneous polarization. The best dielectric and piezoelectric properties of $\varepsilon_{33}^T = 1430$, d_{33} ~365 pC/N and k_p ~50% appear in the ceramic with $x = 0.18$, which is close to the tetragonal side of the MPB. By comparison, Q_m shows a different tendency with changing x. It seems that the Q_m values for the $(1-x)PZ_{56}T_{44}$–xBZT ceramics decrease with increasing BZT content, although the E_c values increases [Fig. 6(b)]. The possible reason is that the formation of phase coexistence tends to make the materials become mechanically softer.

IV. Conclusions

The BZT-substituted $PZ_{56}T_{44}$ solid-solution ceramics has been fabricated by a conventional mixed-oxide method. The phase transition behavior and compositional dependences of electrical properties of $(1-x)PZ_{56}T_{44}$–xBZT ceramics were investigated. An MPB between rhombohedral and tetragonal ferroelectric phases was identified to be in the range of $0.15 < x < 0.18$. With increasing BZT content, the solid solutions were found to exhibit typical dielectric diffuseness and frequency dispersion characteristics. Owing to the coexistence of two ferroelectric phases with different lattice distortions, the $(1-x)PZ_{56}T_{44}$–xBZT ceramics with $x = 0.18$ own optimum dielectric and piezoelectric properties of $\varepsilon_{33}^T = 1430$, $d_{33} = 365$ pC/N, $k_p = 50\%$, $T_c = 260°C$ and $Q_m = 32$. The experimental results demonstrate that this ternary system could be a good piezoelectric material with reduced lead content and interesting electrical properties.

References

[1]B. Jaffe, W. R. Cook, and H. Jaffe, *Piezoelectric Ceramics*. Academic Press, NY, 1971.

[2]G. H. Haertling, "Ferroelectric Ceramics: History and Technology," *J. Am. Ceram. Soc.*, **82** [4] 797–818 (1999).

[3]H. X. Fu and R. E. Cohen, "Polarization Rotation Mechanism for Ultrahigh Electromechanical Response in Single-Crystal Piezoelectrics," *Nature*, **403**, 281–3 (2000).

[4]R. Guo, L. E. Cross, S. E. Park, B. Noheda, D. E. Cox, and G. Shirane, "Origin of the High Piezoelectric Response in $PbZr_{1-X}Ti_XO_3$," *Phys. Rev. Lett.*, **84** [23] 5423–6 (2000).

[5]H. Ouchi, K. Nagano, and S. Hayakawa, "Piezoelectric Properties of Pb$(Mg_{1/3}Nb_{2/3})O_3$-$PbTiO_3$-$PbZrO_3$ Solid Solution Ceramics," *J. Am. Ceram. Soc.*, **48** [12] 630–5 (1965).

[6]H. Q. Fan, G. T. Park, J. J. Choi, J. Ryu, and H. E. Kim, "Preparation and Improvement in the Electrical Properties of Lead-Zinc-Niobate-Based Ceramics by Thermal Treatments," *J. Mater. Res.*, **17** [1] 180–5 (2002).

[7]M. Kondo, M. Hida, K. Omote, O. Taniguchi, T. Mita, S. Umemiya, and K. Kurihara, "Preparation of $PbNi_{1/3}Nb_{2/3}O_3$-$PbTiO_3$-$PbZrO_3$ Ceramic Multilayer Actuator With Silver Internal Electrodes," *Sens. Actuators A*, **109** [1–2] 143–8 (2003).

[8]T. R. Shrout and S. J. Zhang, "Lead-Free Piezoelectric Ceramics: Alternatives for PZT?," *J. Electroceram.*, **19** [1] 111–24 (2007).

[9]A. A. Belik, S. Iikubo, K. Kodama, N. Igawa, S. Shamoto, M. Maie, T. Nagai, Y. Matsui, S. Y. Stefanovich, B. I. Lazoryak, and E. Takayama-Muromachi, "$BiScO_3$: Centrosymmetric $BiMnO_3$-Type Oxide," *J. Am. Chem. Soc.*, **128** [3] 706–7 (2005).

[10]M. M. Kumar, V. R. Palkar, K. Srinivas, and S. V. Suryanarayana, "Ferroelectricity in a Pure $BiFeO_3$ Ceramic," *Appl. Phys. Lett.*, **76** [19] 2764–6 (2000).

[11]T. Atou, H. Chiba, K. Ohoyama, Y. Yamaguchi, and Y. Syono, "Structure Determination of Ferromagnetic Perovskite $BiMnO_3$," *J. Solid State Chem.*, **145** [2] 639–42 (1999).

[12]Y. Inaguma and T. Katsumata, "High Pressure Synthesis, Lattice Distortion, and Dielectric Properties of a Perovskite $Bi(Ni_{1/2}Ti_{1/2})O_3$," *Ferroelectrics*, **286**, 111–7 (2003).

[13]D. D. Khalyavin, A. N. Salak, N. P. Vyshatko, A. B. Lopes, N. M. Olekhnovich, A. V. Pushkarev, I. I. Maroz, and Y. V. Radyush, "Crystal Structure of Metastable Perovskite $Bi(Mg_{1/2}Ti_{1/2})O_3$: Bi-Based Structural Analogue of Antiferroelectric $PbZrO_3$," *Chem. Mater.*, **18** [21] 5104–10 (2006).

[14]M. R. Suchomel, A. M. Fogg, M. Allix, H. J. Niu, J. B. Claridge, and M. J. Rosseinsky, "Bi_2ZnTiO_6: A Lead-Free Closed-Shell Polar Perovskite With a Calculated Ionic Polarization of 150 μC cm^{-2}," *Chem. Mater.*, **18** [21] 4987–9 (2006).

[15]A. A. Belik, T. Wuernisha, T. Kamiyama, K. Mori, M. Maie, T. Nagai, Y. Matsui, and E. Takayama-Muromachi, "High-Pressure Synthesis, Crystal Structures, and Properties of Perovskite-Like $BiAlO_3$ and Pyroxene-Like $BiGaO_3$," *Chem. Mater.*, **18** [1] 133–9 (2006).

[16]P. Baettig, C. F. Schelle, R. LeSar, U. V. Waghmare, and N. A. Spaldin, "Theoretical Prediction of New High-Performance Lead-Free Piezoelectrics," *Chem. Mater.*, **17** [6] 1376–80 (2005).

[17]H. Wang, H. T. Huang, W. Lu, H. L. W. Chan, B. Wang, and C. H. Woo, "Theoretical Prediction on the Structural, Electronic, and Polarization Properties of Tetragonal Bi_2ZnTiO_6," *J. Appl. Phys.*, **105** [5] 053713, 8pp (2009).

[18]T. T. Qi, I. Grinberg, and A. M. Rappe, "First-Principles Investigation of the Highly Tetragonal Ferroelectric Material $Bi(Zn_{1/2}Ti_{1/2})O_3$," *Phys. Rev. B*, **79** [9] 094114, 5pp (2009).

[19]A. A. Belik, S. Y. Stefanovich, B. I. Lazoryak, and E. Takayama-Muromachi, "$BiInO_3$: A Polar Oxide With $GdFeO_3$-Type Perovskite Structure," *Chem. Mater.*, **18** [7] 1964–8 (2006).

[20]M. R. Suchomel and P. K. Davies, "Enhanced Tetragonality in (x) $PbTiO_3$-(1-x)$Bi(Zn_{1/2}Ti_{1/2})O_3$ and Related Solid Solution Systems," *Appl. Phys. Lett.*, **86** [26] 262905, 3pp (2005).

[21]C. C. Huang and D. P. Cann, "Phase Transitions and Dielectric Properties in $Bi(Zn_{1/2}Ti_{1/2})O_3$-$BaTiO_3$ Perovskite Solid Solutions," *J. Appl. Phys.*, **104** [2] 024117, 4pp (2008).

[22]C. C. Huang, N. Vittayakorn, and D. P. Cann, "Structure and Ferroelectric Properties of $Bi(Zn_{1/2}Ti_{1/2})O_3$-$(Bi_{1/2}K_{1/2})TiO_3$ Perovskite Solid Solutions," *IEEE Trans. Ultrason. Ferroelectr. Freq. Control*, **56** [7] 1304–8 (2009).

[23]S. T. Zhang, F. Yan, and B. Yang, "Morphotropic Phase Boundary and Electrical Properties in (1-x)$Bi_{0.5}Na_{0.5}TiO_3$-x$Bi(Zn_{0.5}Ti_{0.5})O_3$ Lead-Free Piezoceramics," *J. Appl. Phys.*, **107** [11] 114110, 4pp (2010).

[24]M. Sutapun, C. C. Huang, D. P. Cann, and N. Vittayakorn, "Phase Transitional Behavior and Dielectric Properties of Lead Free (1-x)$(K_{0.5}Na_{0.5})NbO_3$-x$Bi(Zn_{0.5}Ti_{0.5})O_3$ Ceramics," *J. Alloys Compd.*, **479** [1–2] 462–6 (2009).

[25]S. C. Lee, L. Wang, M. H. Lee, Y. S. Sung, M. H. Kim, T. K. Song, S. S. Kim, J. H. Cho, B. C. Choi, K. S. Choi, and Y. Sakka, "$Bi(Zn_{0.5}Ti_{0.5})O_3$ Substitution Effects in $Pb(Zr,Ti)O_3$ Piezoelectric Ceramics Around Morphotropic Phase Boundary Region," *Ferroelectrics*, **401**, 181–5 (2010).

[26]M. H. Tang, J. Zhang, X. L. Xu, H. Funakubo, Y. Sugiyama, H. Ishiwara, and J. Li, "Electrical Properties and X-ray Photoelectron Spectroscopy Studies of $Bi(Zn_{0.5}Ti_{0.5})O_3$ Doped $Pb(Zr_{0.4}Ti_{0.6})O_3$ Thin Films," *J. Appl. Phys.*, **108** [8] 084101, 5pp (2010).

[27]M. H. Tang, G. J. Dong, Y. Sugiyama, and H. Ishiwara, "Frequency-Dependent Electrical Properties in $Bi(Zn_{0.5}Ti_{0.5})O_3$ Doped $Pb(Zr_{0.4}Ti_{0.6})O_3$ Thin Film for Ferroelectric Memory Application," *Semicond. Sci. Technol.*, **25** [3] 035006, 4pp (2010).

[28]T. T. Wang and J. Yu, "Piezoelectric Properties of $Pb_{0.85}Bi_{0.15}(Zr_{0.442}Ti_{0.483}Zn_{0.075})O_3$ Ceramics," *Ferroelectrics*, **408**, 20–4 (2010).

[29]A. Dwivedi and C. A. Randall, "Morphotropic Phase Boundary in High Temperature Ferroelectric x$Bi(Zn_{1/2}Ti_{1/2})O_3$-Y$PbZrO_3$-Z$PbTiO_3$ Perovskite Ternary Solid Solution," *Mater. Lett.*, **65** [9] 1308–11 (2011).

[30]J. Chen, X. Y. Sun, J. X. Deng, Y. Zu, Y. T. Liu, J. H. Li, and X. R. Xing, "Structure and Lattice Dynamics in $PbTiO_3$-$Bi(Zn_{1/2}Ti_{1/2})O_3$ Solid Solutions," *J. Appl. Phys.*, **105** [4] 044105, 5pp (2009).

[31]I. Grinberg, M. R. Suchomel, P. K. Davies, and A. M. Rappe, "Predicting Morphotropic Phase Boundary Locations and Transition Temperatures in Pb- and Bi-Based Perovskite Solid Solutions From Crystal Chemical Data and First-Principles Calculations," *J. Appl. Phys.*, **98** [9] 094111, 10pp (2005).

[32]O. Khamman, X. Tan, S. Ananta, and R. Yimnirun, "Ferroelectric Properties of (1-x)$Bi(Zn_{1/2}Ti_{1/2})O_3$-X$PbZrO_3$ Ceramics," *J. Mater. Sci.*, **44** [16] 4321–5 (2009).

[33]J. Kelly, M. Leonard, C. Tantigate, and A. Safari, "Effect of Composition on the Electromechanical Properties of (1-x)$Pb(Mg_{1/3}Nb_{2/3})O_3$-X$PbTiO_3$ Ceramics," *J. Am. Ceram. Soc.*, **80** [4] 957–64 (1997).

[34]C. A. Randall, R. Eitel, B. Jones, T. R. Shrout, D. I. Woodward, and I. M. Reaney, "Investigation of a High T_c Piezoelectric System: (1-x)$Bi(Mg_{1/2}Ti_{1/2})O_3$-(x)$PbTiO_3$," *J. Appl. Phys.*, **95** [7] 3633–9 (2004).

[35]S. J. Zhang, C. Stringer, R. Xia, S. M. Choi, C. A. Randall, and T. R. Shrout, "Investigation of Bismuth-Based Perovskite System: (1-x)$BiNi_{2/3}Nb_{1/3}O_3$-X$PbTiO_3$," *J. Appl. Phys.*, **98** [3] 034103, 5pp (2005).

[36]R. E. Eitel, C. A. Randall, T. R. Shrout, and S. E. Park, "Preparation and Characterization of High Temperature Perovskite Ferroelectrics in the Solid-Solution (1-x)$BiScO_3$-X$PbTiO_3$," *Jpn. J. Appl. Phys.*, **41** [4] 2099–104 (2002).

[37]D. M. Lin, K. W. Kwok, K. H. Lam, and H. L. W. Chan, "Structure and Electrical Properties of $K_{0.5}Na_{0.5}NbO_3$-$LiSbO_3$ Lead-Free Piezoelectric Ceramics," *J. Appl. Phys.*, **101** [7] 074111, 6pp (2007).

[38]J. G. Wu, D. Q. Xiao, Y. Y. Wang, J. G. Zhu, P. Yu, and Y. H. Jiang, "Compositional Dependence of Phase Structure and Electrical Properties in $(K_{0.42}Na_{0.58})NbO_3$-$LiSbO_3$ Lead-Free Ceramics," *J. Appl. Phys.*, **102** [11] 114113, 5pp (2007).

[39]K. Uchino and S. Nomura, "Critical Exponents of the Dielectric Constants in Diffused-Phase-Transition Crystals," *Ferroelectrics*, **44**, 55–61 (1982).

[40]A. A. Bokov and Z. G. Ye, "Recent Progress in Relaxor Ferroelectrics With Perovskite Structure," *J. Mater. Sci.*, **41** [1] 31–52 (2006).

[41]H. L. Du, W. C. Zhou, F. Luo, D. M. Zhu, S. B. Qu, and Z. B. Pei, "Phase Structure, Dielectric Properties, and Relaxor Behavior of $(K_{0.5}Na_{0.5})NbO_3$-$(Ba_{0.5}Sr_{0.5})TiO_3$ Lead-Free Solid Solution for High Temperature Applications," *J. Appl. Phys.*, **105** [12] 124104, 6pp (2009).

[42]R. D. Shannon, "Revised Effective Ionic Radii and Systematic Studies of Interatomic Distances in Halides and Chalcogenides," *Acta Crystallogr.*, **32** [5] 751–67 (1976). □